Numerical study of optically induced director oscillations in nematic liquid crystals: Transition to chaos via homoclinic gluings and the role of backflow

G. Demeter*
Research Institute for Particle and Nuclear Physics of the Hungarian Academy of Sciences, Konkoly-Thege Miklós út 29-33, H-1121 Budapest, Hungary

D. O. Krimer and L. Kramer†
Physikalisches Institut der Universität Bayreuth, D-95440 Bayreuth, Germany
(Received 21 May 2005; published 17 November 2005)

We investigate the director oscillations of a homeotropically aligned nematic liquid crystal that are generated by cw laser radiation incident at a slightly oblique angle. The full nematodynamic equations are solved numerically, and it is shown that the inclusion of backflow leads to a qualitative change of the theoretical bifurcation scenario at moderate to high intensities. Very good correspondence is achieved with recent observations. The route to chaos via a sequence of homoclinic gluing bifurcations, whose existence was suggested by simple models, but doubted by recent calculations and experiments, is shown to exist in a parameter region unexplored by experiments.

DOI: 10.1103/PhysRevE.72.051712 PACS number(s): 42.70.Df, 42.65.Sf, 61.30.Gd

Nematic liquid crystals (nematics) have been found to exhibit a great variety of interesting optic phenomena, in particular, those associated with the so-called light-induced director reorientation. Nematics are optically anisotropic materials, their local optical properties (the direction of the optical axis) are determined by the orientation of the director. The electric field of the light wave, on the other hand, exerts a torque on the director, so that intense light can alter the optical properties of the medium it propagates through. This leads to a great variety of nonlinear optical responses of the nematic (see Ref. [1]).

In some cases, the interaction of light and nematic leads to persistent motion of the director. Such a case is when a layer of homeotropically aligned nematic (i.e., the director aligned perpendicular to the layer) is illuminated by a cw laser beam with a small, oblique angle of incidence and a linear polarization that is perpendicular to the plane of incidence (ordinary wave) (Fig. 1). Experiments revealed that the initial oscillations grow more complex as the light intensity is increased, eventually turning chaotic [2,3]. A relatively simple model, derived using perturbation theory [4], was successful in identifying the first few bifurcations of the system. It suggested that the system takes an uncommon route to chaos through a cascade of homoclinic gluing bifurcations [5]. This was very encouraging, as no experimental system was known to exhibit such behavior. Recent experiments [6] made clear that the accuracy of the model is limited—the first gluing bifurcation could be observed, but not a sequence of gluings. A numerical study of the equations was performed [7] and it concluded that the system does not exhibit a cascade of gluing bifurcations. However, considerable discrepancy between its results and those of the experiments remained—most notably, using the parameters that corresponded to the experimental setups of [3,6]; no chaos was found in the simulation at any intensity.

Two major approximations may limit the applicability of both models [4] and simulations [7]. One is that light was considered to be an infinite plane wave, while the experiments were, in fact, performed with laser beams whose transverse size w_0 was about the same as the thickness of the layer L. However, in recent experiments, where the role of the finite beam size was investigated (in a different geometry), it was shown that the bifurcation scenario changes only if $w_0/L \approx 0.5-0.3$ [8], so this approximation seems to be justified. The second approximation is that the flow of the nematic was neglected. In nematic, the director motion is coupled to flow, so any physical effect that reorients the director also induces flow. This is the so-called backflow effect [9]. While having a subordinate role, backflow has been found to qualitatively change the dynamical behavior of the director in electrically driven reorientation [10] and shift bifurcation thresholds in director dynamics induced by circularly polarized light [11]. To the lowest order, backflow can be considered in a theory by renormalizing the rotational viscosity γ_1 [11,12], but this approach is valid only if reorientation is small.

In an attempt to bring the theory and experiment closer and to gain insight into the importance of the backflow effect in this geometry, we have performed a numerical study of the

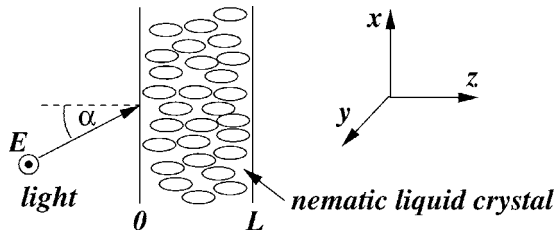

FIG. 1. Geometry of the setup: an ordinary wave incident on a cell of homeotropic nematic at a slightly oblique angle.

*Electronic address: gdemeter@rmki.kfki.hu
†Professor Lorenz Kramer has deceased.

full set of nematodynamic equations that include both director motion and fluid flow. In the absence of temperature gradients and assuming an incompressible fluid, these consist of the Navier-Stokes equation for the velocity field and the equation for the director [9]. (Heating of the nematic by the laser is negligible, even though intensity is high, as the cell is thin, absorption is small, and heat diffuses out quickly.) Assuming that the incident light is an infinite plane wave, and all physical quantities depend only on the z coordinate, the Navier-Stokes equation reduces to

$$\varrho_m \partial_t v_i = -\partial_z T_{iz}^{visc}, \quad i = x,y. \tag{1}$$

Incompressibility and only the z dependence together implies $v_z=0$. ϱ_m is the mass density and T_{ij}^{visc} are components of the viscous stress tensor that are algebraic expressions of the director components and the velocity gradients. The director equations will reduce to

$$\gamma_1 \partial_t n_x + n_z[(\alpha_2 - \gamma_2 n_x^2)\partial_z v_x - \gamma_2 n_x n_y \partial_z v_y] = -h_x^{\perp},$$

$$\gamma_1 \partial_t n_y + n_z[(\alpha_2 - \gamma_2 n_y^2)\partial_z v_y - \gamma_2 n_x n_y \partial_z v_x] = -h_y^{\perp}, \tag{2}$$

where $\mathbf{h}^{\perp}$ is the perpendicular molecular field whose components can be obtained by taking the variational derivatives of the free energy, $h_i = \delta F / \delta n_i$, and projecting this vector to a plane perpendicular to $\mathbf{n}$. F consists of the elastic free energy and the energy the nematic acquires in the electric field of the light due to anisotropic polarizability [1]. n_z can be obtained from $n_i n_i = 1$. For the electric fields we must solve Maxwell's equations with the z-dependent dielectric tensor $\varepsilon_{ij} = \varepsilon_{\perp}\delta_{ij} + \varepsilon_a n_i n_j$.

The material parameters the equations contain are K_1, K_2, K_3 (splay, twist, and bend elastic constants), α_i (six Leslie viscosities, of which only five are independent and which also define $\gamma_2 = \alpha_3 + \alpha_2$ and the rotational viscosity $\gamma_1 = \alpha_3 - \alpha_2$), and $\varepsilon_{\perp}, \varepsilon_a$ (dielectric constant and dielectric anisotropy). In addition, the thickness of the cell L and the wavelength of the light λ are needed. The two control parameters of the theory are the angle of incidence of the light α and the normalized intensity $\rho = I/I_F$. [$I_F = \pi^2 c(\varepsilon_{\perp} + \varepsilon_a)K_3/(L^2 \varepsilon_a \sqrt{\varepsilon_{\perp}})$ is the threshold intensity for the light-induced Fréedericksz transition at normal incidence.]

This system of PDEs contains two characteristic timescales: the momentum diffusion time $\tau_{visc} = \varrho_m L^2/\gamma_1$, which is associated with the relaxation of $\mathbf{v}$, and the characteristic timescale of the director motion $\tau = \gamma_1 L^2/\pi^2 K_3$. Since typically $\tau \sim 1$ s and $\tau_{visc} \sim 10^{-6}$ s, the velocity follows adiabatically the motion of the director, so the inertial terms in Eq. (1) can be neglected. Thus the components of the stress tensor do not depend on z and Eq. (1) can be used to eliminate $\mathbf{v}$ from the director Eq. (2) [11,13]. We then have two coupled equations for n_x, n_y. These will be integrodifferential equations however, due to the elimination procedure and to Maxwell's equations, integrals of functions of n_x, n_y will enter. They can be solved numerically using spatial discretisation and standard ODE solving techniques.

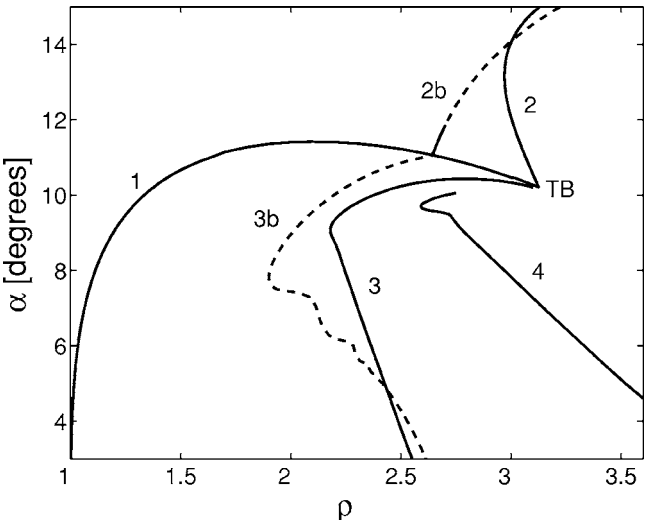

FIG. 2. Bifurcation diagram as a function of the dimensionless intensity ρ and angle of incidence α. The lines are explained in the text. $\rho_{TB}=3.12$, $\alpha_{TB}=10.21°$.

We have explored the behavior of the system as a function of ρ and α. We assume $\mathbf{v}=0$ and $n_x, n_y = 0$ (strong anchoring of the director) at the boundaries. In the calculations we used the known material parameters for the nematic $E7$, which was used in the experiments [3,6], $K_1 = 11.09 \times 10^{-12}$ N, $K_2 = 5.82 \times 10^{-12}$ N, $K_3 = 15.97 \times 10^{-12}$ N [14], $\varepsilon_{\perp} = 2.25$, and $\varepsilon_a = 0.76$ (Merck data sheet). The viscosities, which are not known for $E7$, were taken from the nematic 5CB at 26 °C: $\alpha_1 = -6.6 \times 10^{-3}$, $\alpha_2 = -7.7 \times 10^{-2}$, $\alpha_3 = -4.2 \times 10^{-3}$, $\alpha_4 = 6.34 \times 10^{-2}$, and $\alpha_5 = 6.24 \times 10^{-2}$ (all in units of N s/m^2) [15]. Furthermore, $\lambda = 514.5$ nm and most calculations were done using $L = 50$ μm (some used $L = 75$ μm for comparison with [6]). The data which the simulation produced were values of n_x and n_y at a series of points in space at each timestep. Boundary conditions permit writing these components as $n_x(z,t) = \Sigma_m A_m(t)\sin(m\pi z/L)$, $n_y(z,t) = \Sigma_m B_m(t)\sin(m\pi z/L)$. Clearly, $\{A_i, B_i = 0\}$ corresponds to homogeneous homeotropic orientation (the basic state). Since higher order modes are strongly damped by elasticity (see [1,4]), only the first few amplitudes are important, so the system effectively reduces to a finite-dimensional one. By calculating these amplitudes, we reduced the amount of data to store and obtained quantities that give better insight into the dynamics. They describe the evolution of the director as motion in a low-dimensional phase space and they make it easy to look for various attracting sets. It is important to note that the system is symmetric with respect to inversion of the y axis: $S: y \to -y$. In terms of the amplitudes, this corresponds to $S: \{A_i, B_k\} \to \{A_i, -B_k\}$ and implies that all fixed points, limit cycles, etc. are either invariant under S, or appear in pairs that are symmetric conjugates of each other.

Figure 2 shows the most important bifurcation lines on the (ρ, α) plane and Fig. 3 depicts some limit cycles at $\alpha = 5°$ and various intensities for $L = 50$ μm. Line 1-2 is the line of primary instability, where the basic state becomes unstable (this is the light-induced Fréedericksz transition). It consists of two sections, which join in a Takens-Bogdanov

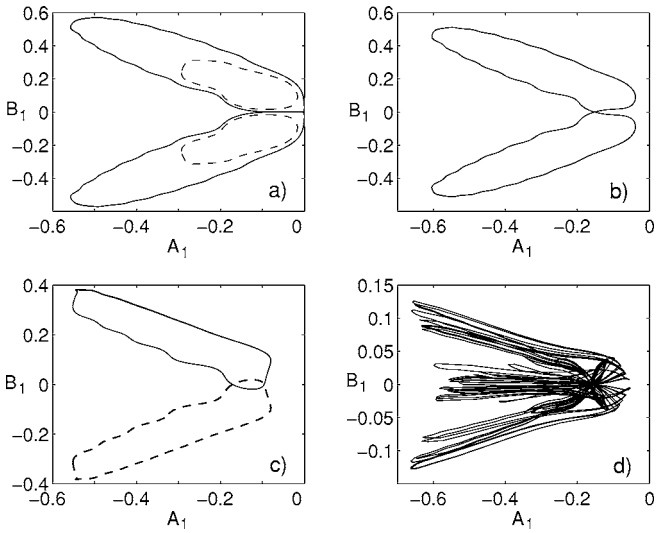

FIG. 3. Limit cycles at $\alpha=5°$ and various intensities: (a) $\rho=2.1$ (dashed lines) and $\rho=2.426$ (solid lines), (b) $\rho=3.0$, (c) $\rho=3.8$ (both solid and dashed lines), and (d) $\rho=4.4$.

point (TB). For small angles the basic state loses stability in a pitchfork bifurcation (line 1), for larger angles in a Hopf bifurcation (line 2). At the pitchfork instability, two new stationary states (fixed points) are created (mutual images under S). As ρ is increased, they lose stability in a secondary Hopf bifurcation (not shown in Fig. 2), where two, symmetry-degenerate limit cycles are created [see Fig. 3(a), dashed lines]. Line 3 in Fig. 2 is the line of the first gluing bifurcation. At this point, the limit cycles are homoclinic orbits to the basic state, which is now a saddle [Fig. 3(a), solid lines] and above the gluing they join to form a single, symmetric, double-length limit cycle [Fig. 3(b)]. This is not a period doubling bifurcation however, as the period diverges as the bifurcation is approached. As ρ is increased, the symmetric limit cycle again becomes homoclinic to the basic state at a certain ρ (line 4, Fig. 2). Above this, it breaks up into two asymmetric limit cycles [Fig. 3(c)]. These, however, are "interlaced," i.e., one loop passes through the other in phase space. Above this bifurcation, there is a great variety of complex and eventually chaotic behavior to be found, but the precise scenario depends on α. At $\alpha=5°$ a strange attractor appears abruptly [Fig. 3(d)].

To assess the importance of backflow, we can compare these results with those obtained in [7], where backflow was neglected. The sequence of the first three bifurcations is the same in both cases, but bifurcation thresholds can differ considerably. In Fig. 2, the dashed lines 2(b) and 3(b) depict the lines of the primary Hopf- and the first-gluing bifurcation respectively, as calculated without flow. [The line of the pitchfork instability (line 1) is unaffected.] The Takens-Bogdanov point is also shifted considerably. The line of the second-gluing bifurcation (where the symmetric limit cycle breaks up as the intensity is increased) does not exist in the calculation without the flow, and neither does the chaotic behavior found at high intensities and $\alpha<8.5°$. Thus, we can say that the flow acquires decisive importance near the first-gluing bifurcation.

This sequence of bifurcations, and director behavior between them corresponds exactly to the various regimes found in the experiments. In [3] stationary reorientation was observed up to $\rho=1.41$ after the primary instability, above which an oscillatory state was found up to $\rho=2.19$. By comparison, with the same parameters ($L=50$ μm and $\alpha=5°$) our simulation showed that the pitchfork instability, which leads to a distorted stationary state, is followed by the secondary Hopf bifurcation at $\rho_H=1.31$. Above this we have a pair of limit cycles. In [3] an intermittent regime was observed between $\rho=2.19$–2.4, where the director was found to switch randomly between oscillation and rotation about the laser incidence plane. In the simulation one can identify this as the vicinity of the first-gluing bifurcation that occurs at $\rho_{g1}=2.42$. Random fluctuations in the experiment cause the intermittent switching between the two limit cycles as the system approaches the gluing. Then a rotation of the director was observed between $\rho=2.4$–2.81, which, in the simulation, corresponds to motion along the double-length, symmetric limit cycle born in the first gluing. Between $\rho=2.81$ and 2.92 a second intermittent regime of director oscillation and rotation was observed, which can be interpreted as the vicinity of the second-gluing bifurcation at $\rho_{g2}=3.52$ in our calculation. The oscillatory regime observed between $\rho=2.92$ and 3.65 corresponds to periodic motion along one of the asymmetric limit cycles above the second gluing in the simulation. Finally, chaotic oscillation was observed in the experiment above $\rho=3.65$, while we have a strange attractor in our calculation above $\rho_{chaos}=4.375$.

A similar sequence of bifurcations was observed in [6] (with $L=75$ μm and $\alpha=5°$), where a reconstruction of the attractors in phase space from the experimental data provides even more convincing proof that the various limit cycles and bifurcations follow each other in the same sequence as in our calculations. First stationary reorientation was between $\rho=1$ and 1.6 (simulation: $\rho_H=1.47$), then an oscillatory regime up to $\rho=1.9$. Between $\rho=1.9$ and 2.0 the system was seen to switch randomly between two oscillatory states (simulation: $\rho_{g1}=2.36$). Another periodic regime was observed between $\rho=2.0$ and 2.6, after which the vicinity of another gluing bifurcation was seen. This was not well resolved though and above $\rho=3.0$, chaotic oscillations were found. In our simulations $\rho_{g2}=3.31$ and $\rho_{chaos}=4.12$. Above the second gluing the two limit cycles are not as well separated as below the first gluing, so random transitions between them may be present in the experiment due to noise even below the onset of true chaos. We note that the bifurcation thresholds obtained in our simulations lie mostly within 10–25 % of the experimental values, which is fairly good, taking into account that the exact viscosities of the material were not known.

An important question is the possible existence of the full cascade of gluing bifurcations leading to chaos, which would make this system unique from the point of view of the basic chaos theory. Scanning the ρ-α plane, we have indeed located a region where this sequence of events takes place, however, it is quite far from the parameters that the experiments were performed with.

Figure 4 shows the first steps of the sequence. As bifurcation lines are nearly parallel to the ρ axis in this region, they are traversed by keeping the intensity fixed at $\rho=2.9$ and decreasing the angle of incidence. After the pitchfork-

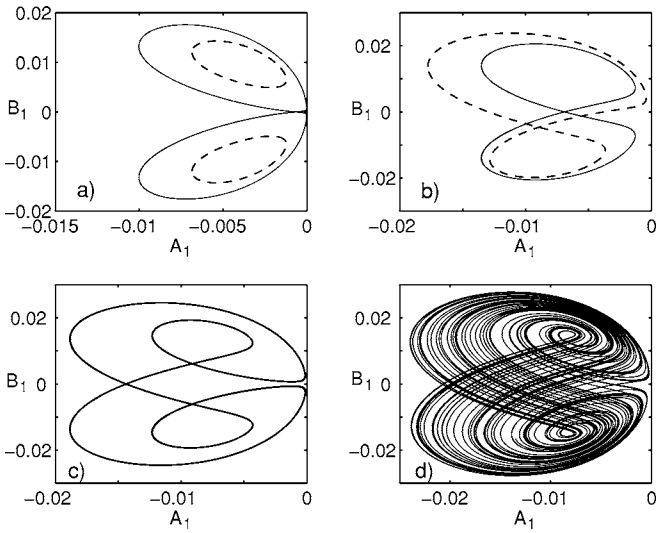

FIG. 4. Limit cycles for a 50 μm thick sample at $\rho=2.9$ and various angles of incidence: (a) $\alpha=10.45°$ (dashed line) and $\alpha=10.408°$ (solid line), (b) $\alpha=10.35°$ (solid line) and $\alpha=10.31°$, (dashed line), (c) $\alpha=10.3°$, and (d) $\alpha=10.25°$.

and the secondary Hopf-bifurcations, we have a pair of limit cycles [dashed lines in Fig. 4(a)] and at $\alpha=10.408°$ we have the first gluing bifurcation [solid line in Fig. 4(a)]. The symmetric, double-length limit cycle [solid line in Fig. 4(b)] then loses stability and two asymmetric limit cycles are born [dashed line in Fig. 4(b), only one of the pair is shown.] These two merge in the next gluing to make a quadruple-length symmetric limit cycle [Fig. 4(c)]. The series of symmetry-breaking instabilities followed by gluings that restore the symmetry continues and we eventually have a strange attractor [Fig. 4(d)]. Clearly, experimental detection of the scenario is challenging, as the range of angles and the director reorientation is small. Furthermore, there is a great variety of complex behavior in this region close to the Takens-Bogdanov point and bifurcation lines lie close to each other. However, taking a thinner sample should improve the chances of detection, as the angle between successive bifurcations and reorientation can both grow considerably.

In conclusion, our simulations prove that to describe dynamical behavior of nematic excited by the light correctly, one has to include a proper treatment of backflow. The present simulations show perfect qualitative correspondence with existing experimental observations at all intensities, and fairly good quantitative agreement. This proves that the flow does play an important role in the dynamical behavior at moderate to high intensities, causing a significant change of the bifurcation scenario. An agreement with observations also seems to justify neglect of finite beamsize effects in this geometry for $w_0 \approx L$, similar to [8]. Furthermore, the uncommon route to chaos via a sequence of homoclinic gluing-bifurcations, whose existence was doubted by experiments and recent calculations [7] was also found, in a parameter region unexplored by experiment.

Financial support by the Deutsche Forschungsgemeinschaft under Contract Nos. Kr 690/16 and 436UNG113/151/1 is gratefully acknowledged.

[1] N. V. Tabiryan, A. V. Sukhov and B. Ya. Zel'dovich, Mol. Cryst. Liq. Cryst. **136**, 1 (1985); F. Simoni, *Nonlinear Optical Properties of Liquid Crystals* (World Scientific, Singapore, 1997).

[2] A. S. Zolotko *et al.*, Liq. Cryst. **15**, 787 (1993); G. Cipparrone, V. Carbone, C. Versace, C. Umeton, R. Bartolino, and F. Simoni, Phys. Rev. E **47**, 3741 (1993).

[3] E. Santamato, P. Maddalena, L. Marrucci, and B. Piccirillo, Liq. Cryst. **25**, 357 (1998).

[4] G. Demeter and L. Kramer, Phys. Rev. Lett. **83**, 4744 (1999); G. Demeter, Phys. Rev. E **61**, 6678 (2000).

[5] A. Arneodo, P. Coullet, and C. Tresser, Phys. Lett. **81A**, 197 (1981); Y. Kuramoto and S. Koga, *ibid.* **92A**, 1 (1982); D. V. Lyubimov and M. A. Zaks, Physica D **9**, 52 (1983).

[6] G. Russo, V. Carbone and G. Cipparrone, Phys. Rev. E **62** 5036 (2000); V. Carbone, G. Cipparrone and G. Russo, *ibid.* **63** 051701 (2001).

[7] G. Demeter and L. Kramer, Phys. Rev. E **64**, 020701(R) (2001); E. Brasselet, *ibid.* **72**, 013701 (2005)

[8] E. Brasselet, B. Doyon, T. V. Galstian, and L. J. Dubé, Phys. Rev. E **69**, 021701 (2004).

[9] P. G. de Gennes and J. Prost, *The Physics of Liquid Crystals* (Clarendon Press, Oxford, 1993).

[10] D. W. Berreman, J. Appl. Phys. **46**, 3746 (1975); C. Z. van Doorn, *ibid.* **46**, 3738 (1975); S. A. Jewell and J. R. Sambles, Appl. Phys. Lett. **84**, 46 (2004).

[11] D. O. Krimer, G. Demeter and L. Kramer, Phys. Rev. E **71**, 051711 (2005).

[12] L. Marrucci, G. Abbate, S. Ferraiuolo, P. Maddalena, and E. Santamato, Mol. Cryst. Liq. Cryst. Sci. Technol., Sect. A **237**, 39 (1993).

[13] B. L. Winkler, H. Richter, I. Rehberg, W. Zimmerman, L. Kramer, and A. Buka, Phys. Rev. A **43**, 1940 (1991).

[14] A. Vella, B. Piccirillo, and E. Santamato, Phys. Rev. E **65**, 031706 (2002).

[15] A. Buka and L. Kramer, *Pattern Formation in Liquid Crystals* (Springer, Berlin, 1995).